Water Quality Research Journal

Water Quality Research Journal Vol 58 No 4, 247 doi: 10.2166/wqrj.2023.111

Phosphorus removal and recovery from anaerobic bioreactor effluent using a batch electrocoagulation process

Gyana Prakash Bhoi [a,*], Kripa S. Singh [a,b] and Dennis A. Connor [a,b]

[a] Department of Civil Engineering, University of New Brunswick, Fredericton, Canada
[b] Department of Chemical Engineering, University of New Brunswick, Fredericton, Canada
*Corresponding author. E-mail: b.gyanaprakash@unb.ca

GPB, 0000-0002-6211-2142

ABSTRACT

A batch monopolar electrocoagulation system was developed and studied for the removal of phosphorus from anaerobic bioreactor effluent using iron as an electrode material. The study focused on the optimization of the independent variables, such as initial pH, retention time (RT), current density (CD) and inter-electrode distance (IED) using the response surface methodology (RSM) to maximize the removal of total phosphorus (TP). A quadratic model was fitted to the experimental data for TP removal. The optimal parameters were found to be pH of 6.75, RT of 11.06 min, CD of 300 A/m^2, and inter-electrode distance of 1.5 cm resulting in 98.05% TP removal and energy consumption of 1.28 kWh/m^3. A kinetic study for TP removal revealed that at optimal conditions, removal followed first-order kinetics ($K = 0.185$ m/min). Phosphorus was recovered from the post-precipitated sludge through combustion at 900 °C followed by acid leaching with sulfuric acid. Acid leaching tests were carried out with sulfuric acid for the post-precipitated sludge obtained at the optimum conditions. It resulted in around 91% of phosphorus recovery at a liquid-to-solid ratio of 100 mL/g.

Key words: central composite design, electrocoagulation, phosphorus recovery, statistical optimization

HIGHLIGHTS

- Effect of calcium in iron-electrocoagulation system.
- Statistical optimization of parameters to maximize total phosphorus removal from anaerobic effluent.
- Consideration of interactive effects of independent variables in process optimization.

GRAPHICAL ABSTRACT

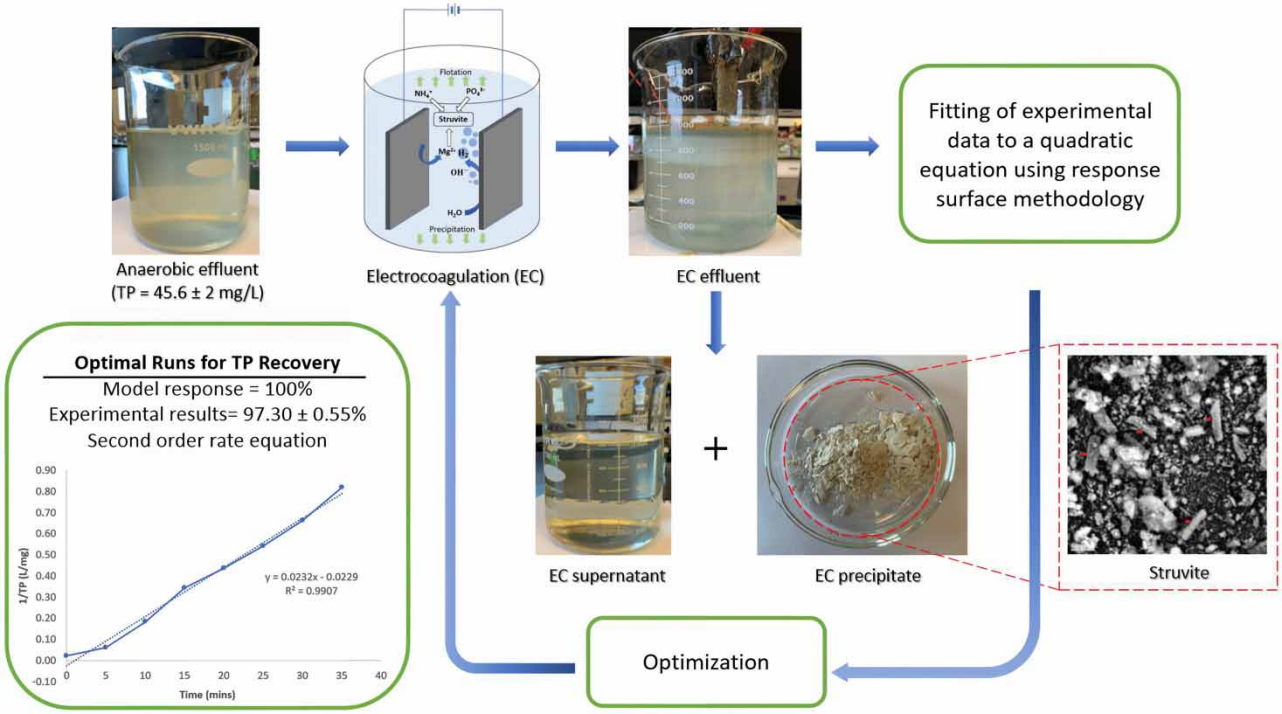

INTRODUCTION

Global phosphorus consumption has gradually increased from 43.7 million tonnes in 2015 to 48.2 million tonnes in 2019 due to the growing demand for food production (Hermann *et al.* 2018). The agricultural sector accounts for 85% of phosphorous consumption (Johnston *et al.* 2014). As phosphate is a limited and nonrenewable resource, a rapid increase in phosphate consumption can put enormous strain on global phosphate rock reserves. It is estimated that the worldwide phosphate reserves will be depleted in 10 decades if the current rate of phosphate mining continues and no alternative measures are adopted (Gilbert 2009). To deal with the scarcity of phosphorus, it is crucial to identify alternate phosphorus sources. Phosphorus levels in typical anaerobically treated wastewater effluents and digestates are generally high (>40 mg/L) (Moerman *et al.* 2009; Huang *et al.* 2017). The recovery of phosphate from these waste streams is an appealing option for achieving long-term phosphorus supplies which otherwise would be discharged into the water environment causing adverse impacts. It has the potential to supply up to one-fifth of worldwide phosphorus demand (Yuan *et al.* 2012).

Agricultural runoff is the major contributor of phosphorus in water bodies. The presence of phosphorus above 0.02 mg/L in the water bodies causes eutrophication, which interferes with the reproduction of algae and microorganisms (Wan *et al.* 2020). This leads to the depletion of dissolved oxygen and generates toxins in the water, resulting in the death of aquatic organisms and causing damage to wildlife (Conley *et al.* 2009; Li *et al.* 2016) and can become a public health concern. The presence of phosphorus in the waste stream encourages the fouling of water pipes, resulting in costly maintenance (Attour *et al.* 2014). Therefore, removal or possible recovery of phosphate from wastewater discharges is crucial to maintain a balance of phosphorus in the aquatic environment, keeping in mind the aspects of sustainable development, and resource recovery.

Conventional methods such as chemical and biological phosphorus recovery methods are widely used industrially and can achieve a low phosphorus concentration (<1 mg/L) in the treated effluent (Yin *et al.* 2015; Wang *et al.* 2018; Li *et al.* 2019). However, chemical precipitation needs large amounts of chemical additives and is associated with high sludge production, whereas biological phosphorus removal is energy-intensive and complex in nature (Sengupta *et al.* 2015). Furthermore, the phosphorus content of the sludge produced by biological phosphorus removal is extremely low (2–3%) (Jupp *et al.* 2021). These shortcomings sparked the interest of researchers in exploring other alternatives for sustainable phosphorus recovery

from anaerobic effluent. Recent studies on phosphorus removal and recovery using an electrochemical membrane (Kekre *et al.* 2021), electrochemical precipitation (Bakshi *et al.* 2020; Govindan *et al.* 2021; Li *et al.* 2021), and microbial fuel cell (Ye *et al.* 2019) are found to be promising. Among these methods, electrochemical precipitation (electrocoagulation) has gained considerable research interest due to its ease of use and high removal efficiency (up to 99%) (Lacasa *et al.* 2011).

Several studies on phosphorus removal using an electrocoagulation system have been published, in the majority of the studies, synthetic wastewater was used, which avoids the effect of organics and other constituent ions on phosphorus removal (Gharibi *et al.* 2010; Zhang *et al.* 2018; Bakshi *et al.* 2020; Zeng *et al.* 2021). To the best of our knowledge, the interaction of parameters such as pH and current density (CD), CD and retention time (RT) were not taken into account in studies using anaerobic effluents from industries (Tran *et al.* 2012; Huang *et al.* 2017). These parameters and their interactions might affect the mass of metal ion generation from the anode. Furthermore, consideration of the interactive effects in process optimization could decrease energy consumption, thereby lowering operational costs. Therefore, further research is warranted for addressing these gaps in the literature. This will help to achieve the desired phosphorus concentration in the effluent to meet discharge guidelines and can serve as a sustainable phosphorus source to meet global phosphorus demand while protecting the environment.

During electrocoagulation, metal ions are generated from the anode under the application of electric current. These metal ions (M^{z+}) react with the phosphate ions present in the effluent, resulting in the formation of insoluble precipitates (Huang *et al.* 2017). Formation of metal hydroxide and polyhydroxides compounds takes place which causes destabilization and aggregation of colloidal substances. The generation of hydrogen at the cathode propels flocs to the water surface (Figure 1).

The dominant reactions for iron as an electrode material are as follows (Linares-Hernández *et al.* 2010; Bernal-Martínez *et al.* 2013):

Anode reaction:

$$Fe(s) \rightarrow Fe^{2+}(aq) + 2e^{-} \quad (1)$$

$$Fe(s) \rightarrow Fe^{3+}(aq) + 3e^{-} \quad (2)$$

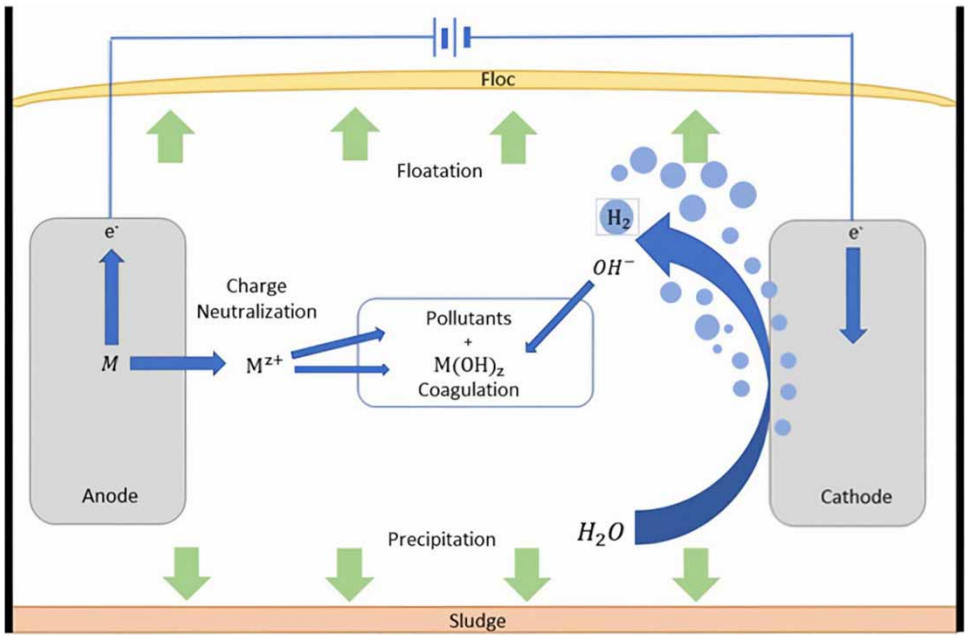

Figure 1 | Mechanism of electrocoagulation.

Cathode reaction:

$$2H_2O(l) + 2e^- \rightarrow H_2(g) + 2OH^-(aq) \quad (3)$$

Formation of compounds such as $Fe_3(PO_4)_2$, $Fe(OH)_2$ and $Fe(OH)_3$ can take place in the bulk solution according to the following reactions.

$$Fe(aq) + 2H_2O(l) \rightarrow Fe(OH)_2(s) + 2H^+(aq) \quad (4)$$

$$4Fe^{2+}(aq) + 10H_2O(l) + O_2(g) \rightarrow 4Fe(OH)_3(s) + 8H^+ \quad (5)$$

$$3Fe^{2+}(aq) + 2PO_4^{3-}(aq) \rightarrow Fe_3(PO_4)_2(s) \quad (6)$$

$$Fe^{3+}(aq) + PO_4^{3-}(aq) \rightarrow FePO_4(s) \quad (7)$$

Phosphorus present in electrocoagulation sludge is bound to metal ions and requires additional processing for phosphorus extraction (Kyle & McClintock 1995). Available methods of phosphorus extraction from phosphorus-rich sludge include biological leaching (Mehta *et al.* 2015), hydroxyapatite precipitation (Lee *et al.* 2018), and leaching (Petzet *et al.* 2012; Atienza-Martínez *et al.* 2014; Damaraju *et al.* 2019; Monea *et al.* 2020). Among the various available methods of phosphorus recovery, leaching is considered economical. The combustion of sludge enhances the availability of phosphorus for recovery. The melting temperature of iron-rich sewage sludge ash ranges between 900 and 1,160 °C (Shao *et al.* 2007; Wang *et al.* 2012). Combustion of post-precipitated electrocoagulation sludge at a melting temperature of 900 °C results in the formation of acid-soluble phosphorus and acid-insoluble iron compounds like iron oxides (Fe_2O_3) from iron phosphate (Damaraju *et al.* 2019).

In this study, a batch monopolar iron-electrocoagulation reactor was developed to investigate the feasibility of phosphorus removal from anaerobic bioreactor effluent. The objectives of this study were to evaluate the effect of process variables (pH, RT, CD, inter-electrode distance (IED)) and their interaction on TP removal, to optimize the parameters for maximizing the TP removal efficiency, to develop a quadratic model for the response prediction using response surface methodology (RSM), and to evaluate the effect of liquid-to-solid (L/S) ratios on phosphorus extraction by acid leaching. Experimental runs were conducted at the optimized run condition and the observed phosphorus removal efficiency was compared with the predicted removal efficiency. The kinetics of TP removal was investigated to determine the rate of phosphorus removal. Acid leaching was used for the sludge obtained from the electrocoagulation system at optimized parameters to recover phosphorus.

MATERIALS AND METHODS

Sampling of the wastewater

Anaerobic bioreactor effluent was collected from an industrial wastewater treatment plant (McCain Foods, Florenceville-Bristol, Canada). The WWTP uses a large covered anaerobic lagoon for the treatment of its wastewater and to generate biogas. The collected sample was stored under 2 °C to avoid degradation of the organic matter present in it. The collected anaerobic bioreactor effluent was homogenized for initial characterization.

Experimental setup and procedure

The reaction was carried out in a batch reactor, with a working volume of 1 L. Iron electrodes of active surface area of 20 cm^2 each having dimensions of width, 4 cm, height, 5 cm, and thickness, 0.06 cm. Two electrodes were connected to a DC power source (GPC-3060D, GWINSTEK, Taiwan) which had a variable output of 0–120 V. A schematic of the experimental setup is presented in Figure 2. The formation of the metal oxides was observed on the surface of the anode after each run. This is referred to as electrode passivation, and it results in increased electricity consumption. The electrodes were scraped after each run using abrasive paper followed by rinsing it several times with distilled water. All experiments were carried out at room temperature (22 °C).

The physico-chemical characteristics of the anaerobic bioreactor effluent are shown in Table 1. The analysis to characterize the effluent was performed in triplicate. Determination of pH, conductivity, total phosphorus (TP), total dissolved solids

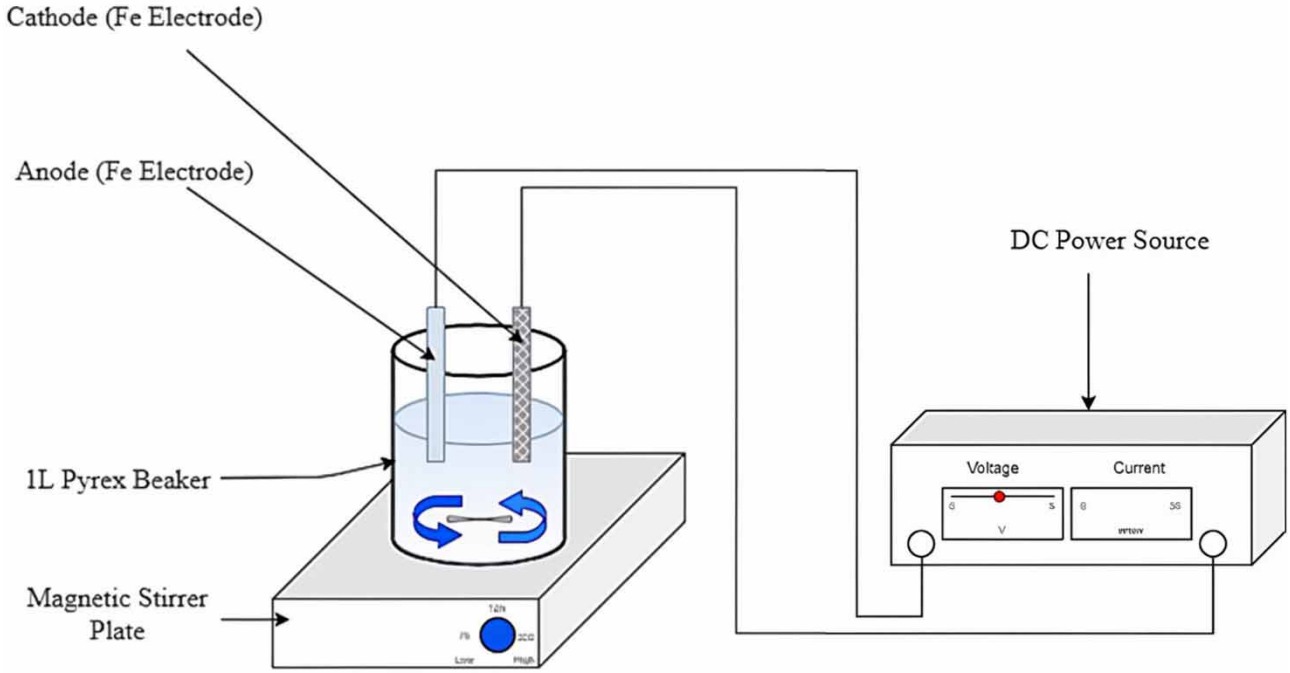

Figure 2 | Schematic of the EC batch reactor setup.

Table 1 | Initial characteristics of the filtered anaerobic bioreactor effluent

Parameter	Unit	Value
pH	–	7.5 ± 0.25
Conductivity	mS/cm	2.7 ± 0.09
fCOD	mg/L	119.1 ± 5
TP	mg/L	45.6 ± 2
NH_3-N	mg/L	141.5 ± 2.5
Ca	mg/L	70.9 ± 2
Mg	mg/L	12 ± 0.5
Na	mg/L	96.4 ± 3

(TDS), total suspended solids (TSS), calcium, magnesium, iron, and filtered chemical oxygen demand (fCOD) was conducted according to Standard Methods (APHA AWWA & WEF 2005). TP, calcium (Ca^{2+}), magnesium (Mg^{2+}), iron (Fe), and sodium (Na^{+}) were measured using ICP-OES (VISTA-MPX Axial, Varian, Australia). The orthophosphate concentration was measured using UV spectrophotometer (DR 2700, HACH, USA). The orthophosphate (PO_4^{3-}) concentration agrees with the TP (PO_4-P) concentration divided by the value 0.3261, as suggested by the Hach methods. The pH was adjusted using NaOH (50%) or HCl (37%). A digital pH meter (AB15, Fisher Scientific, USA) was used to measure the pH. Constant stirring was done using a magnetic stirrer. Anaerobic bioreactor effluent was filtered through glass fiber filters (Whatman, 47 mm) with a pore size of 1.2 μm to eliminate the effects of suspended solids in the experiment. During each run, samples of 10 mL were collected from the surface at an interval of 2.5 min and filtered through cellulose acetate membrane filters (Whatman, 47 mm) with a pore size of 0.45 μm. The filtrate was acidified using ACS-grade nitric acid for elemental analysis. Electrocoagulation effluent was centrifuged to separate flocs and precipitate from the treated effluent. This precipitate was oven dried at 105 °C for X-ray diffraction (XRD), energy-dispersive spectroscopy (EDS), and scanning electron microscopy (SEM).

The removal efficiency was calculated using Equation (8).

$$\text{Removal efficiency (\%)} = \frac{C_i - C_f}{C_i} \times 100 \tag{8}$$

Here C_i and C_f are the initial and final concentrations of TP.

The mass of production of metal ions by the anodic dissolution can be calculated using Faraday's law as shown in the following equation.

$$m = \frac{ItM}{zF} \tag{9}$$

Here, m represents the mass of the metal ions generated in grams, I represents the current in amperes, t represents the treatment time in seconds, M represents the material's molar mass in g/mol, z represents the valency of the produced ion (for iron, $z = 2$), F represents the Faraday's constant (96,500 C/mol). However, this equation does not consider electrode surface conditions.

Energy consumption is critical in electrochemical processes because electricity is the energy source. This is a parameter used to determine the process's applicability. Energy consumption under optimal conditions was determined by the following equation.

$$\text{Energy consumption}\left(\text{KW.}\frac{\text{h}}{\text{m}^3}\right) = \frac{E \times I \times t}{V \times 1,000} \tag{10}$$

Here E denotes the voltage in volts, I denotes the current applied in amperes, t denotes the RT in hours, and V denotes the volume of the effluent treated in m^3.

Recovery of phosphorus from the post-precipitated electrocoagulation sludge was performed by combustion at 900 °C followed by acid leaching. Acid leaching tests were conducted with sulfuric acid with an acid load of 100 kg/kg P and various liquid-to-solid ratios (50, 100, 150, and 200 mL/g) (Atienza-Martínez *et al.* 2014). Experiments were conducted in duplicate. The samples were collected after 24 h for analysis.

Experimental design and model development

The variables affecting TP removal were optimized using RSM. Run parameters for this study were obtained using Minitab software (version 20, Minitab Inc., USA). The independent process variables for this study are initial pH (pH), RT, CD and IED. A central composite design (CCD) with five levels (−2, −1, 0, 1, 2) was used to assess the effect of the independent variables and their interaction on the dependent variable. Table 2 presents the independent variables and levels as defined by the CCD design. For this study, TP removal efficiency was chosen as the response. The ranges of the independent process variables were determined by preliminary studies. The number of experiments needed for this study was determined by the following equation:

$$N = 2^K + 2K + C_0 \tag{11}$$

where N is the number of experiments, K is the number of factors, and C_0 is the number of central points. The CCD for 4

Table 2 | Independent variables and levels

Variables	$-2(\alpha)$	−1	0	+1	$+2(\alpha)$
pH	3	4.75	6.5	8.25	10
RT (min)	5	7.5	10	12.5	15
Current density (A/m^2)	100	150	200	250	300
IED (cm)	0.5	0.75	1	1.25	1.5

factors with 7 central points involves 31 experimental runs. Table 3 lists the design matrix and run parameters as per the CCD. Multiple regression analysis was carried out using Minitab Software to fit the experimental data to a quadratic model. This quadratic model describes the correlation between factors and the response variable. ANOVA was carried out for the statistical validation of the model and to maximize the removal of TP. This study used response surface and contour plots to analyze the interactive effects among factors. The *p*-value was used to assess the lack of fit. Nonsignificant model terms were eliminated for a better fit.

RESULTS AND DISCUSSION

Statistical analysis

Thirty-one experimental runs were carried out in duplicate as per CCD, for modeling the TP removal. The results obtained from the ANOVA are represented in Table 4. The significance of model terms was evaluated using the *p*-value. A *p*-value of

Table 3 | Design matrix including experimental and predicted values

	Variables				TP removal efficiency (%)	
Run order	pH	RT	CD	IED	Experimental	Predicted
1	−1 (4.75)	−1 (7.5)	−1 (150)	−1 (0.75)	7.47	8.76
2	1 (8.25)	−1 (7.5)	−1 (150)	−1 (0.75)	72.83	72.64
3	−1 (4.75)	1 (12.5)	−1 (150)	−1 (0.75)	36.08	37.91
4	1 (8.25)	1 (12.5)	−1 (150)	−1 (0.75)	91.28	93.04
5	−1 (4.75)	−1 (7.5)	1 (250)	−1 (0.75)	34.58	37.47
6	1 (8.25)	−1 (7.5)	1 (250)	−1 (0.75)	84.07	80.15
7	−1 (4.75)	1 (12.5)	1 (250)	−1 (0.75)	67.43	66.61
8	1 (8.25)	1 (12.5)	1 (250)	−1 (0.75)	96.94	100.55
9	−1 (4.75)	−1 (7.5)	−1 (150)	1 (1.25)	27.09	22.97
10	1 (8.25)	−1 (7.5)	−1 (150)	1 (1.25)	71.50	73.31
11	−1 (4.75)	1 (12.5)	−1 (150)	1 (1.25)	36.08	40.58
12	1 (8.25)	1 (12.5)	−1 (150)	1 (1.25)	86.00	82.19
13	−1 (4.75)	−1 (7.5)	1 (250)	1 (1.25)	61.69	60.51
14	1 (8.25)	−1 (7.5)	1 (250)	1 (1.25)	92.41	89.66
15	−1 (4.75)	1 (12.5)	1 (250)	1 (1.25)	78.45	78.13
16	1 (8.25)	1 (12.5)	1 (250)	1 (1.25)	98.83	98.54
17	−2 (3)	0 (10)	0 (200)	0 (1)	5.40	3.41
18	2 (10)	0 (10).	0 (200)	0 (1)	85.77	87.69
19	0 (6.5)	−2 (5)	0 (200)	0 (1)	42.06	45.18
20	0 (6.5)	2 (15)	0 (200)	0 (1)	86.40	83.21
21	0 (6.5)	0 (10)	−2 (100)	0 (1)	49.23	47.73
22	0 (6.5)	0 (10)	2 (300)	0 (1)	91.35	92.78
23	0 (6.5)	0 (10)	0 (200)	−2 (0.5)	76.51	74.66
24	0 (6.5)	0 (10)	0 (200)	2 (1.5)	82.39	86.85
25	0 (6.5)	0 (10)	0 (200)	0 (1)	77.38	80.76
26	0 (6.5)	0 (10)	0 (200)	0 (1)	80.13	80.76
27	0 (6.5)	0 (10)	0 (200)	0 (1)	81.71	80.76
28	0 (6.5)	0 (10)	0 (200)	0 (1)	79.96	80.76
29	0 (6.5)	0 (10)	0 (200)	0 (1)	85.69	80.76
30	0 (6.5)	0 (10)	0 (200)	0 (1)	80.65	80.76
31	0 (6.5)	0 (10)	0 (200)	0 (1)	82.47	80.76

Table 4 | ANOVA results

Source	DF	Adj SS	Adj MS	*F*-value	*p*-value	Remarks
Model	14	19,639.7	1,402.8	111.40	0.000	Significant
Linear	4	16,092.6	4,023.1	319.47	0.000	Significant
A	1	10,656.6	10,656.6	846.22	0.000	Significant
B	1	2,168.6	2,168.6	172.20	0.000	Significant
C	1	3,044.6	3,044.6	241.77	0.000	Significant
D	1	222.9	222.9	17.70	0.001	Significant
Square	4	2,627.2	656.8	52.16	0.000	Significant
A*A	1	2,235.7	2,235.7	177.54	0.000	Significant
B*B	1	499.9	499.9	39.69	0.000	Significant
C*C	1	203.2	203.2	16.14	0.001	Significant
D*D	1	4.0	4.0	0.32	0.579	Not significant
2-Way interaction	6	919.9	153.3	12.18	0.000	Significant
A*B	1	76.4	76.4	6.07	0.025	Significant
A*C	1	449.3	449.3	35.68	0.000	Significant
A*D	1	183.1	183.1	14.54	0.002	Significant
B*C	1	0.2	0.2	0.01	0.909	Not significant
B*D	1	132.9	132.9	10.55	0.005	Significant
C*D	1	78.1	78.1	6.20	0.024	Significant
Error	16	201.5	12.6	–	–	–
Lack-of-fit	10	161.9	16.2	2.45	0.142	Not significant
Pure error	6	39.6	6.6	–	–	–
Total	30	19,841.2	–	–	–	–

less than 0.05 indicates that the independent variable has a significant influence on the response. The results showed that 12 out of the 14 model terms were found to be significant for TP removal efficiency. This includes linear terms such as pH (A), RT (B), CD (C), and IED (D), as well as squared terms such as pH^2 (A^2), RT^2 (B^2), CD^2(C^2), and interaction terms such as pH · RT (AB), pH · CD (AC), pH · IED (AD), RT · IED (BD), CD · IED (CD). The lack-of-fit test for the TP removal efficiency (p-value = 0.142) was found to be nonsignificant. A high R^2 value signifies a good fit for the experimental data to the model. $R^2_{\text{predicted}}$ value indicates the ability of the model to predict the response for a given set of operating conditions. After the removal of statistically insignificant terms, the modified quadratic model for TP removal efficiency was obtained as the following equation.

$$\begin{aligned}\text{Total phosphorus removal efficiency}(\%) &= 80.76 + 21.072\text{pH} + 9.506\text{RT} + 11.263\text{CD} + 3.047\text{IED} \\ &- 8.802\text{pH}^2 - 4.141\text{RT}^2 - 2.626\text{CD}^2 - 2.185\text{pH} \cdot \text{RT} \\ &- 5.299\text{pH} \cdot \text{CD} - 3.383\text{pH} \cdot \text{IED} - 2.882\text{RT} \cdot \text{IED} + 2.209\text{CD} \cdot \text{IED} \end{aligned} \quad (12)$$

According to ANOVA results, the coefficient of determination was found to be 0.99. It signifies that the statistical model can explain 98.96% of the variability in the response. In this study for the removal of TP, the R^2 (0.99) value is fairly close to the adjusted R^2 (0.98) and predicted R^2 (0.96) values indicate that the model is valid. (Makwana & Ahammed 2017). The model summary is shown in Table 5. Figure 3 demonstrates the plot of actual vs predicted TP removal efficiency.

The model equation includes linear terms, quadratic terms, and interaction terms explaining the relationship of factors with the response variable. Initial pH was found to be the most important factor among linear and squared terms affecting TP removal. The interaction of initial pH and CD was found to be the most significant interaction term affecting the response.

Table 5 | Model summary

Parameter	R^2	Adjusted R^2	Predicted R^2	P_{lof} (lack of fit)
Total phosphorus	98.96	98.27	96.27	0.142

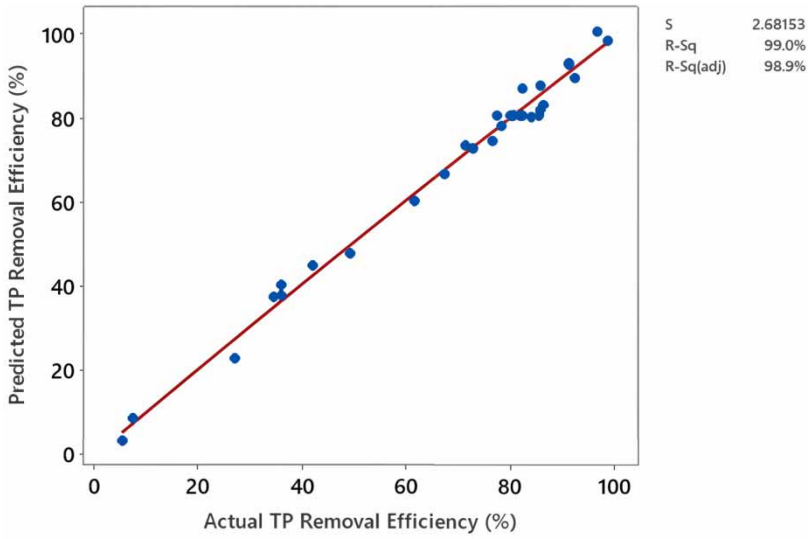

Figure 3 | Predicted vs actual TP removal efficiency.

For the main effect, a positive coefficient indicates that TP removal increases as the main effect increases, whereas a negative value would indicate that TP removal decreases as the main effect decreases.

Effect of independent process variables

Initial pH

The Initial pH of the solution is a critical factor for the removal and recovery of TP from wastewater. It affects the conductivity of the anaerobic effluent and anodic dissolution. TP removal efficiency was low under highly acidic conditions and gradually increased with an increase in pH. It denotes that the phosphorus removal mechanism is strongly influenced by the initial pH of the solution. Phosphate tends to precipitate as ferric phosphate ($FePO_4$) at acidic pH due to a lack of hydroxide ions (OH^-). During the electrocoagulation process, the solution pH increases due to the formation of OH^- ions. Whereas at a higher pH range (>7), the formation of ferric hydroxide ($Fe(OH)_3$) occurs. Ferric hydroxide acts as an adsorbent that provides active sites for the adsorption of phosphate (Sincero & Sincero 2003). Huang *et al.* (2017) discovered that phosphorus recovery from anaerobic bioreactor effluent using an iron-electrocoagulation system decreases as the initial pH increases, whereas Damaraju *et al.* (2020) discovered that removal efficiency increases as the pH approaches neutral. However, interference of calcium ions in the iron-electrocoagulation system for phosphorus removal has not been observed so far. During the experiments, the formation of hydroxyapatite was observed at alkaline conditions (pH > 7.5). In this study, TP removal was found to be increasing with an increase in pH up to 9. Further increase in the initial pH of the solution leads to electrode passivation thereby causing a decrease in removal efficiency. Electrode passivation can be reduced with electrode polarity reversal. Higher removal efficiency at alkaline pH can be justified in terms of phosphorus adsorption by ferric hydroxide and the formation of calcium phosphate.

Current density

The CD has a significant impact on the rate of electrocoagulation process (Bektaş *et al.* 2004). According to Faraday's law, an increase in CD causes an increase in the production of metal ions (coagulants), resulting in higher phosphorus recovery (Dolati *et al.* 2017). Furthermore, as CD increases, the rate of bubble formation increases while the size of the bubble

decreases. Both effects are advantageous for high pollutant removal via H_2 flotation (Holt *et al.* 2002; Kobya *et al.* 2006). Within a CD range of 100–300 A/m^2, the phosphorus removal efficiency is found to increase with increasing CD.

Retention time

TP removal efficiency is found to be increasing with an increase in RT up to 12.5 min. For a given CD, the mass of the coagulant added from the anode into the solution is directly proportional to the RT as shown in Equation (10). Furthermore, a longer RT allows enough time for the reaction to occur under the continuous addition of metal ions (Ramcharan & Bissessur 2017). Further increase in RT beyond 12.5 min had a negligible effect on the removal efficiency because enough metal ions were already present in the solution. This observation is in agreement with other findings (Lacasa *et al.* 2011; Attour *et al.* 2014; Bakshi *et al.* 2020; Damaraju *et al.* 2020)

Inter-electrode distance

IED is an important factor affecting the performance of electrocoagulation systems. Within a range of 0.5–1.5 cm, the efficiency of phosphorus removal was found to be increasing with an increase in IED. The maximum phosphorus removal was observed at an IED of 1.5 cm. At a low IED (1 cm), movement of colloids and fluid through the electrode gap is obstructed resulting in the accumulation of precipitates on the electrode surfaces. As a result, electrical resistance increases (Phalakornkule *et al.* 2009). Furthermore, colloidal particle interaction taking place at a low IED affects flotation and settling of the precipitates which leads to increased resistance and affects TP removal (Sridhar *et al.* 2011; Shankar *et al.* 2014).

Variable interaction and response

Response surface and contour plots were created changing the two factors and keeping another two factors constant (Center point). The significance of linear, squared, and interaction terms is determined by comparing the corresponding *p*-values from the ANOVA results. For two-factor interactions, the relationship between the interaction terms and the response is explained using response surfaces and contour plots. Figures 4 and 5 depict the plots of the response of the TP removal efficiency to the interaction terms. According to the interactive effect of pH and RT, the efficiency of TP removal increased with an increase in pH and RT, as shown in Figures 4(a) and 5(a). Figure 5(a) shows that when the pH is in the range of 6.5–10 and the RT is greater than 8.5 min, more than 90% removal efficiency can be achieved. Figures 4(b) and 5(b) depict the interaction plots for pH and CD. These plots show that TP removal efficiency increases with increasing pH and CD. Removals of more than 90% are shown in Figure 5(b) for pH ranges 6.5–10 and current densities greater than 175 A/m^2. The interaction plot of pH and IED are depicted in Figures 4(c) and 5(c). It illustrates a higher removal efficiency at a pH range of 7.5–10 which is independent of IED.

According to the interaction plot of RT and IED described in Figures 4(d) and 5(d), TP removal increases with an increase in RT. The higher removal efficiency was observed in Figure 5(d) at retention times greater than 11 min, and this was independent of IED. The interaction plots for CD and IED are depicted in Figures 4(e) and 5(e). The higher removal efficiency was observed when the CD was greater than 200 A/m^2 and the IED was greater than 0.87 cm.

Effect on COD removal

The electrocoagulation process can remove a variety of contaminants from wastewater, including nutrients, suspended solids, and organic matter and improves the water quality of the treated effluent (Emamjomeh & Sivakumar 2009). The concentration of organic matter in an aqueous solution is typically expressed by COD. According to the study carried out by Li & Sheng (2021), an increase in organic matter resulted in a decrease in soluble Fe^{2+} ions in the aqueous solution. The primary reason for this claim was that organic matter removal during electrocoagulation occurs as a result of coagulation by Fe^{2+} or adsorption on the surface of ferric hydroxide. This resulted in coagulant (Fe^{2+} ions) consumption by organic matter in the wastewater, making it a limiting factor for phosphorus removal.

The effect of the iron-electrocoagulation system on COD removal was investigated using factorial plots generated with Minitab. Factorial plots describe the relationship between the process variables and the response. The initial pH of the solution influences the stability of the metal hydroxide compounds formed during the reaction as well as the efficiency of COD removal. The COD removal efficiency was found to increase with increasing pH from 3 to 10. The factorial plot for the initial pH shown in Figure S1(a) shows that high COD removal can be achieved for the iron electrode under alkaline conditions. Similar findings were observed by Ebba *et al.* (2021) for a pH range of 3–7.5. During this study, an increase in RT resulted in an increase in COD removal efficiency (Figure S1(b)). COD removal was found to increase with increasing CD, as illustrated

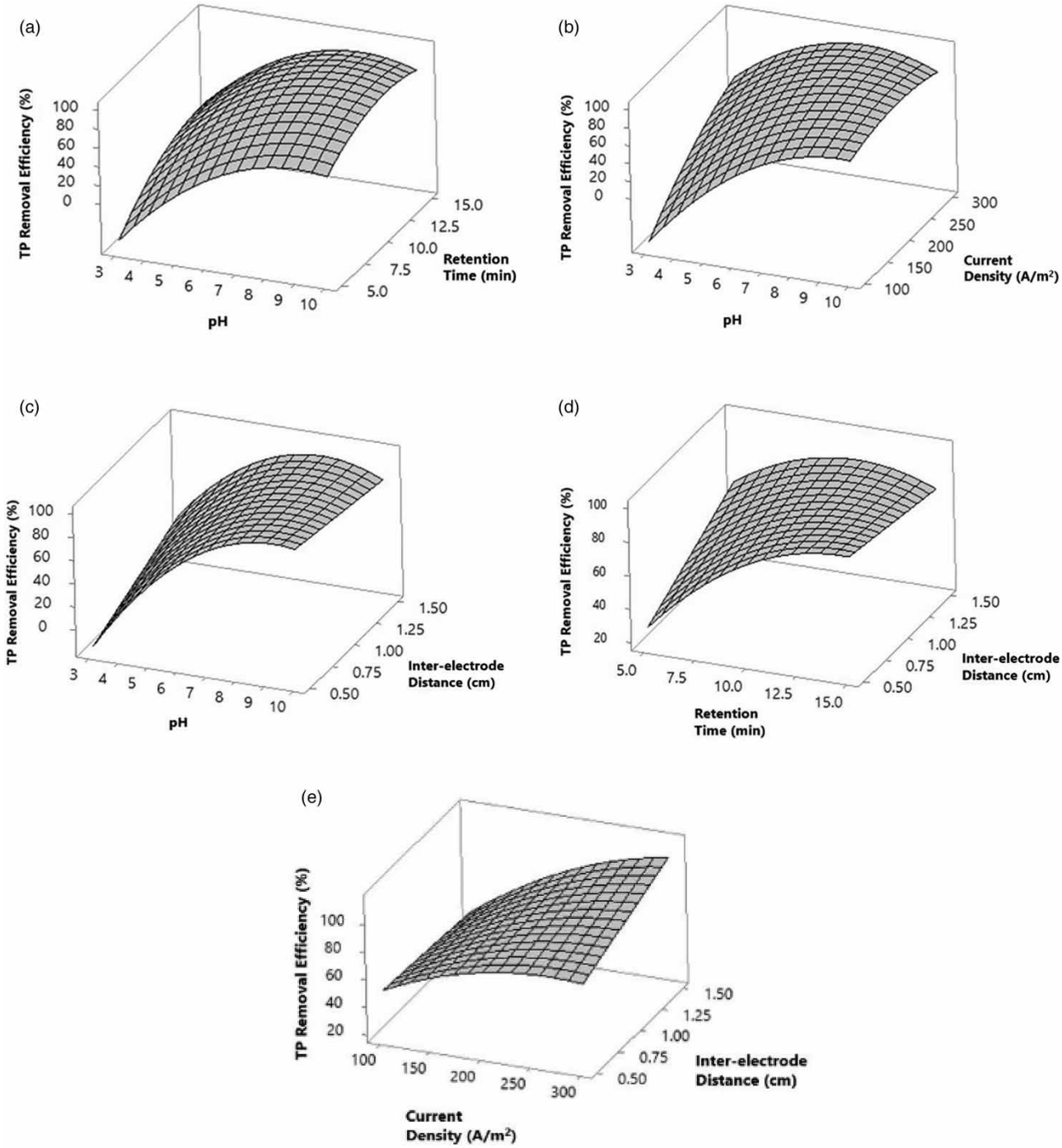

Figure 4 | Response surface plots for TP removal: (a) pH and RT, (b) pH and CD, (c) pH and IED, (d) RT and IED, (e) CD and IED.

in Figure S1(c). However, increasing the CD above 250 A/m^2 resulted in a decrease in COD removal efficiency. This could be because electrode passivation occurs at high CD, resulting in a decrease in metal ion addition. Increased COD removal with an increase in RT and CD is due to an increase in the addition of metal ions and hydroxyl ions into the solution. An increase in IED between 0.5 and 1.5 cm has no effect on COD removal efficiency. The factorial plot for IED is shown in Figure S1(d). However, when compared to 0.5 and 1.5 cm inter-electrode distances, 1 cm IED resulted in low COD removal.

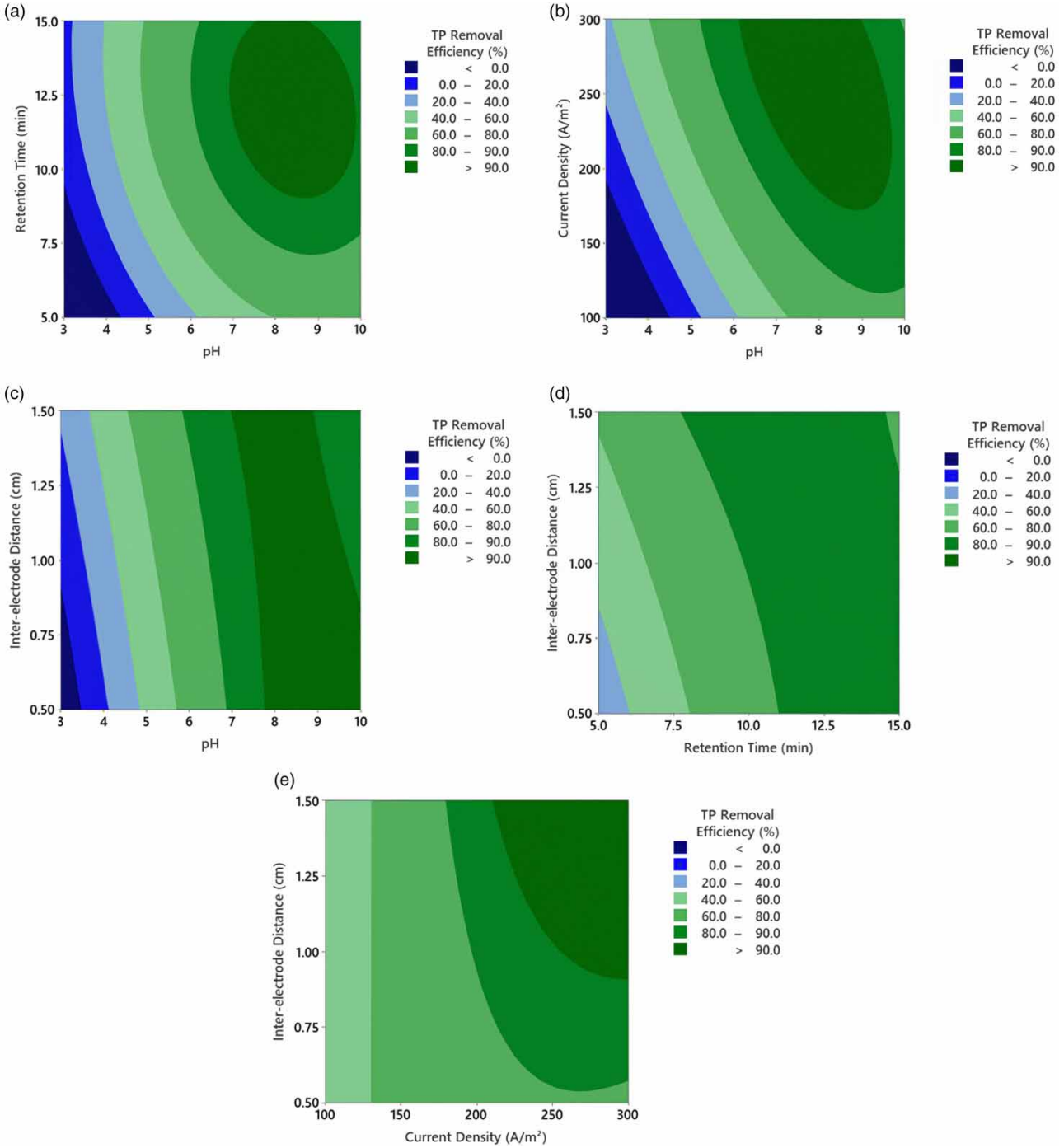

Figure 5 | Contour plots for TP removal: (a) pH and RT, (b) pH and CD, (c) pH and inter-electrode distance, (d) RT and IED, (e) CD and IED.

Optimization

Optimized conditions for the TP removal efficiency were obtained after evaluating the significance of independent process variables. The factors affecting TP removal were optimized using MiniTab software (version 20). This study found that optimal conditions are a pH of 6.75, an RT of 11.06 min, a CD of 300 A/m^2 and an IED of 1.5 cm. At the optimum conditions, the model predicts that all the phosphorus present in the anaerobic bioreactor effluent will be removed. Confirmation runs were

Table 6 | Verification of experimental results at optimal conditions

Optimum conditions	TP removal efficiency (%)
Model response	100
Experimental results	98.05
Error	1.95
Standard deviation	±0.75

pH = 6.75, RT = 11.06 min, CD = 300 A/m^2, IED = 1.5 cm, V = 11.57 V.

performed using the model's predicted optimal conditions. Table 6 displays the experimental results under optimal conditions.

Electrocoagulation sludge of 276 ± 11 mg was obtained from a liter of anaerobic effluent during the optimal electrocoagulation runs. XRD analysis of the sludge was carried out to find out the presence of crystalline compounds. The results as shown in Figure S2 show the amorphous nature of the sludge. EDS analysis of the sludge shown in Figure S3 revealed the presence of C, O, P, Cl, Ca, and Fe as primary elements. The presence of phosphorus indicates that it has been successfully adsorbed onto iron hydroxides. The formation of amorphous structures with large grooves (binding sites) was revealed by SEM image (Figure S4) of the sludge.

TP removal under experimental conditions was found to be 98.05%, which agrees with the predicted response. At optimal conditions, the energy consumption was determined to be 1.28 kWh/m^3. The efficacy of the electrocoagulation system for phosphorus removal in this study was compared to the optimization conditions of previously conducted studies treating various types of wastewaters (Table 7).

Kinetics of TP removal

The kinetics of phosphorus removal were studied, with the experimental runs carried out under optimal conditions (pH = 6.75, RT = 11.06 min, CD = 300 A/m^2, IED = 1.5 cm). The rate equation for phosphorus removal from the anaerobic effluent has been expressed using the given first-order rate law (13).

$$-V\left(\frac{dC}{dt}\right) = KAC \tag{13}$$

Table 7 | Efficacy of EC on various types of wastewater

Serial No	Type of wastewater	Optimum conditions				Electrode material	Removal efficiency (%)	References
		pH	RT (mins)	Current density/Current/ Voltage	IED (cm)			
1	Sludge anaerobic supernatant	3	80	37.5 A/m^2	2	Fe	99	Huang *et al.* (2017)
2	Municipal wastewater	7	20	382 A/m^2	1	Mild steel	97	Tran *et al.* (2012)
3	Palm oil mill effluent	6.4	7.69	77.8 A/m^2	–	Fe	73	Damaraju *et al.* (2019)
4	Synthetic	7	14	11.5 V	3	Scrap Al	90	Bakshi *et al.* (2020)
5	Dairy manure	7.4	100	0.6 A	4	Low carbon steel	96.7	Zhang *et al.* (2016)
6	Synthetic	5.5	40	40 V	1.5	Fe	>99	Gharibi *et al.* (2010)
7	Synthetic	7.4	34	21 A/m^2	1.8	Fe	90.24	Zeng *et al.* (2021)
8	Anaerobic bioreactor effluent	6.75	11.06	300 A/m^2	1.5	Fe	98.05	Present Study

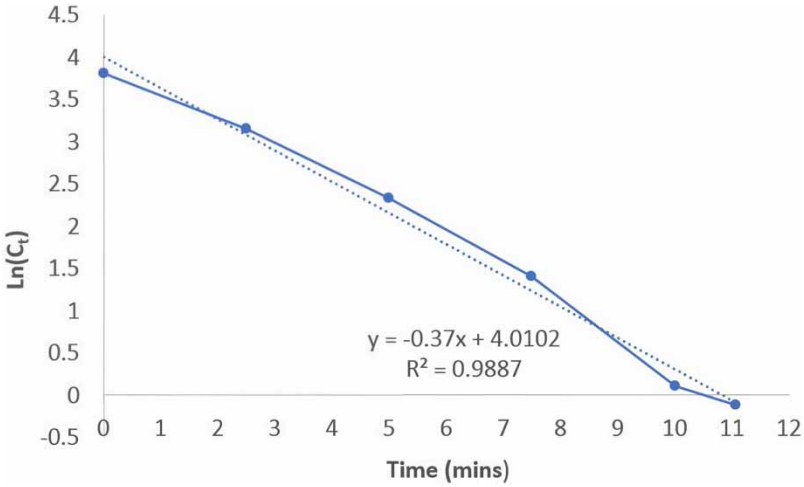

Figure 6 | Ln(C_t) vs time.

According to İrdemez *et al.* (2006), the preceding equation can be expressed as Equation (14)

$$V \ln\left(\frac{C_i}{C_t}\right) = KAt \tag{14}$$

$$\ln(C_t) = \left(\frac{-KA}{V}\right)t + \ln(C_i) \tag{15}$$

Here, V denotes the volume of the effluent treated, C_i denotes the initial phosphorus concentration and C_t denotes the phosphorus concentration at any given time, K denotes the reaction rate constant, and A is the sacrificial surface area of the anode. The variation of TP concentration with time is shown in Figure 6. It describes that the kinetic data for the phosphorus recovery is well fitted by the first-order rate equation. The rate constant for phosphorus removal at optimal conditions was 0.185 m/min.

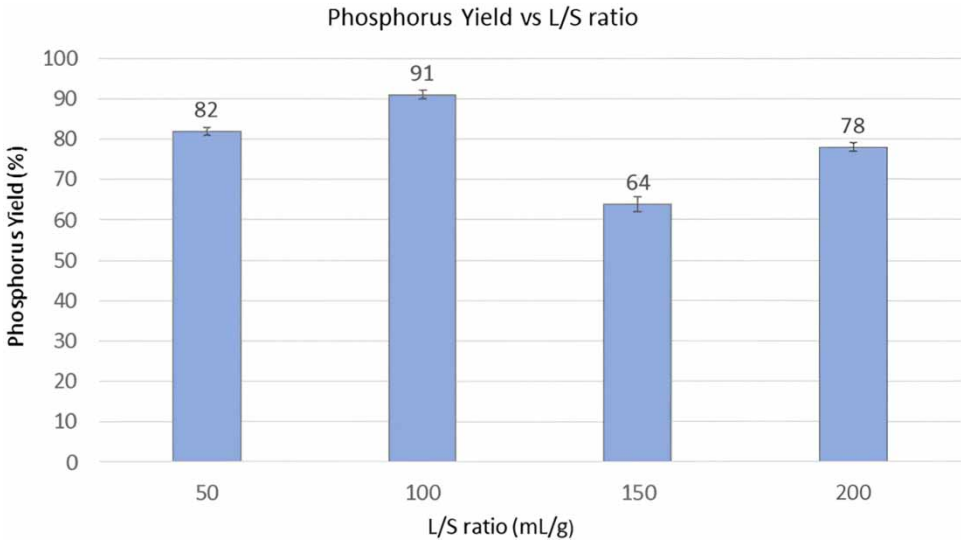

Figure 7 | Effect of *L/S* ratio on phosphorus yield using sulfuric acid.

Acid leaching

Acid-leaching tests were carried out using sulfuric acid. Sulfuric acid is widely used in industry for phosphorus extraction from phosphate rock due to its high strength and proton-donating ability (Atienza-Martínez *et al.* 2014). The leaching of phosphorus at an acid load of 100 kg/kg P and various liquid-to-solid (L/S) ratios are shown in Figure 7. It represents phosphorus yield for sludge combusted at 900 °C. This sludge ash has a phosphorus content of 15.97 $\pm$ 0.72% by mass. At an acid load of 100 kg/kg P and an L/S ratio of 100 mL/g, phosphorus recovery of more than 90% was observed. When the L/S ratio increased to 150 mL/g, the phosphorus concentration in the leachate decreased. The observed phosphorus recovery was greater than 75% for an L/S ratio of 200 mL/g. For an L/S ratio of 50 mL/g, a phosphorus recovery of 82% was observed. The concentration of sulfuric acid affects the acid-leaching process. The molarity of sulfuric acid decreases as the liquid-to-solid ratio increases while the acid load remains constant. The dissolution of phosphorus in the leachate is influenced by the solution pH and L/S ratio. As an acid's molarity increases, its pH decreases. A decrease in pH causes an increase in phosphorus dissolution for a post-precipitated electrocoagulation sludge (Monea *et al.* 2020). An increase in the liquid-to-solid ratio for a constant sulfuric acid concentration causes an increase in phosphorus solubility for the post-precipitated electrocoagulation sludge over a 24-h period (Damaraju *et al.* 2019). The phosphorus dissolution is affected by changes in the L/S ratio and molarity of the acid simultaneously. In this study, an L/S ratio of 100 mL/g was found to be optimal.

CONCLUSIONS

In this study, a monopolar electrocoagulation reactor was developed to investigate the feasibility of the removal and recovery of phosphorus from the effluent of an anaerobic bioreactor treating industrial wastewaters. The response surface method was used to investigate and model the effects of independent process variables. The statistical optimization predicted complete (100%) removal of phosphorus at the optimum condition of pH of 6.75, RT of 11.06 min, CD of 300 A/m^2, and IED of 1.5 cm, whereas the removal of 98.05% was observed during experimental conditions. Energy consumption at optimized conditions was found to be 1.28 kWh/m^3. The batch monopolar system is efficient in removing phosphorus from the anaerobic bioreactor effluent. A kinetic study for TP removal at optimal conditions revealed that the TP removal rate was well fitted to the first-order rate model. Acid leaching data show that the maximum phosphorus recovered from the post-precipitated sludge ash is 91% at a liquid-to-solid ratio of 100 mL/g. More research should be carried out to study the electrode passivation and the effect of electrode polarity reversal on the performance of electrocoagulation reactors.

ACKNOWLEDGEMENTS

The authors are thankful for the funding support provided by the Natural Sciences and Engineering Research Council (NSERC) of Canada, New Brunswick Innovation Foundation, and the University of New Brunswick. The authors are grateful to Steve Cogswell at the University of New Brunswick's Microscopic and Microanalysis Facility for SEM and Ven Reddy for XRD at the University of New Brunswick's Geochemical and Spectrographic Facility.

DATA AVAILABILITY STATEMENT

All relevant data are included in the paper or its Supplementary Information.

CONFLICT OF INTEREST

The authors declare there is no conflict.

REFERENCES

APHA/AWWA/WEF. 2005 *Standard Methods for the Examination of Water and Wastewater*. 21st edn. APHA-AWWA-WEF (American Public Health Association, Eaton, A. D., American Water Works Association, & Water Environment Federation), Washington, DC.

Atienza–Martínez, M., Gea, G., Arauzo, J., Kersten, S. R. A. & Kootstra, A. M. J. 2014 Phosphorus recovery from sewage sludge char ash. *Biomass and Bioenergy* **65**, 42–50.

Attour, A., Touati, M., Tlili, M., Ben Amor, M., Lapicque, F. & Leclerc, J.-P. 2014 Influence of operating parameters on phosphate removal from water by electrocoagulation using aluminum electrodes. *Separation and Purification Technology* **123**, 124–129. https://doi.org/10.1016/j.seppur.2013.12.030.

Bakshi, A., Verma, A. K. & Dash, A. K. 2020 Electrocoagulation for removal of phosphate from aqueous solution: statistical modeling and techno-economic study. *Journal of Cleaner Production* **246**, 118988. https://doi.org/10.1016/j.jclepro.2019.118988.

Bektaş, N., Akbulut, H., Inan, H. & Dimoglo, A. 2004 Removal of phosphate from aqueous solutions by electro-coagulation. *Journal of Hazardous Materials* **106** (2), 101–105. https://doi.org/10.1016/j.jhazmat.2003.10.002.

Bernal-Martínez, L. A., Barrera-Díaz, C., Natividad, R. & Rodrigo, M. A. 2013 Effect of the continuous and pulse in situ iron addition onto the performance of an integrated electrochemical–ozone reactor for wastewater treatment. *Fuel* **110**, 133–140. https://doi.org/10.1016/j.fuel.2012.11.067.

Conley, D. J., Paerl, H. W., Howarth, R. W., Boesch, D. F., Seitzinger, S. P., Havens, K. E., Lancelot, C. & Likens, G. E. 2009 Controlling eutrophication: Nitrogen and phosphorus. *Science* **323** (5917), 1014–1015.

Damaraju, M., Yoshihara, H., Bhattacharyya, D., Panda, T. K. & Kurilla, K. K. 2019 Phosphorus recovery from the sludge generated from a continuous bipolar mode electrocoagulation (CBME) system. *Water Science and Technology: A Journal of the International Association on Water Pollution Research* **79** (7), 1348–1356. https://doi.org/10.2166/wst.2019.131.

Damaraju, M., Bhattacharyya, D., Panda, T. K. & Kurilla, K. K. 2020 Downstream processing of palm oil mill effluent in a CBME reactor. *Journal of Hazardous, Toxic, and Radioactive Waste* **24** (1), 04019040.

Dolati, M., Aghapour, A. A., Khorsandi, H. & Karimzade, S. 2017 Boron removal from aqueous solutions by electrocoagulation at low concentrations. *Journal of Environmental Chemical Engineering* **5** (5), 5150–5156.

Ebba, M., Asaithambi, P. & Alemayehu, E. 2021 Investigation on operating parameters and cost using an electrocoagulation process for wastewater treatment. *Applied Water Science* **11** (11), 175. https://doi.org/10.1007/s13201-021-01517-y.

Emamjomeh, M. M. & Sivakumar, M. 2009 Review of pollutants removed by electrocoagulation and electrocoagulation/flotation processes. *Journal of Environmental Management* **90** (5), 1663–1679. https://doi.org/10.1016/j.jenvman.2008.12.011.

Gharibi, H., Mahvi, A. H., Chehrazi, M., Sheikhi, R. & Hosseini, S. S. 2010 Phosphorous removal from wastewater effluent using electro-coagulation by aluminum and iron plates. *Analytical and Bioanalytical Electrochemistry* **2** (3), 165–177. Scopus.

Gilbert, N. 2009 Environment: The disappearing nutrient. *Nature* **461** (7265), 716–718.

Govindan, K., Im, S.-J., Muthuraj, V. & Jang, A. 2021 Electrochemical recovery of H2 and nutrients (N, P) from synthetic source separate urine water. *Chemosphere* **269**, 129361. https://doi.org/10.1016/j.chemosphere.2020.129361.

Hermann, L., Kraus, F. & Hermann, R. 2018 Phosphorus processing – potentials for higher efficiency. *Sustainability* **10** (5), Article 5. https://doi.org/10.3390/su10051482.

Holt, P. K., Barton, G. W., Wark, M. & Mitchell, C. A. 2002 A quantitative comparison between chemical dosing and electrocoagulation. *Colloids and Surfaces A: Physicochemical and Engineering Aspects* **211** (2), 233–248. https://doi.org/10.1016/S0927-7757(02)00285-6.

Huang, H., Zhang, D., Zhao, Z., Zhang, P. & Gao, F. 2017 Comparison investigation on phosphate recovery from sludge anaerobic supernatant using the electrocoagulation process and chemical precipitation. *Journal of Cleaner Production* **141**, 429–438. https://doi.org/10.1016/j.jclepro.2016.09.127.

İrdemez, Ş., Yildiz, Y. Ş. & Tosunoğlu, V. 2006 Optimization of phosphate removal from wastewater by electrocoagulation with aluminum plate electrodes. *Separation and Purification Technology* **52** (2), 394–401. https://doi.org/10.1016/j.seppur.2006.05.020.

Johnston, A. E., Poulton, P. R., Fixen, P. E. & Curtin, D. 2014 Chapter Five - Phosphorus: Its efficient use in agriculture. In Advances in Agronomy Vol. 123 (Sparks, D. L., ed.). Cambridge, MA: Academic Press, pp. 177–228.

Jupp, A. R., Beijer, S., Narain, G. C., Schipper, W. & Slootweg, J. C. 2021 Phosphorus recovery and recycling – closing the loop. *Chemical Society Reviews* **50** (1), 87–101. https://doi.org/10.1039/D0CS01150A.

Kekre, K. M., Anvari, A., Kahn, K., Yao, Y. & Ronen, A. 2021 Reactive electrically conducting membranes for phosphorus recovery from livestock wastewater effluents. *Journal of Environmental Management* **282**, 111432. https://doi.org/10.1016/j.jenvman.2020.111432.

Kobya, M., Demirbas, E., Can, O. T. & Bayramoglu, M. 2006 Treatment of levafix orange textile dye solution by electrocoagulation. *Journal of Hazardous Materials* **132** (2), 183–188. https://doi.org/10.1016/j.jhazmat.2005.07.084.

Kyle, M. A. & McClintock, S. A. 1995 The availability of phosphorus in municipal wastewater sludge as a function of the phosphorus removal process and sludge treatment method. *Water Environment Research* **67** (3), 282–289.

Lacasa, E., Cañizares, P., Sáez, C., Fernández, F. J. & Rodrigo, M. A. 2011 Electrochemical phosphates removal using iron and aluminium electrodes. *Chemical Engineering Journal* **172** (1), 137–143. https://doi.org/10.1016/j.cej.2011.05.080.

Lee, C.-G., Alvarez, P. J. J., Kim, H.-G., Jeong, S., Lee, S., Lee, K. B., Lee, S.-H. & Choi, J.-W. 2018 Phosphorous recovery from sewage sludge using calcium silicate hydrates. *Chemosphere* **193**, 1087–1093.

Li, C. & Sheng, Y. 2021 Organic matter affects phosphorus recovery during vivianite crystallization. *Water Science and Technology* **83**(8), 2038–2050.

Li, R., Wang, J. J., Zhou, B., Awasthi, M. K., Ali, A., Zhang, Z., Lahori, A. H. & Mahar, A. 2016 Recovery of phosphate from aqueous solution by magnesium oxide decorated magnetic biochar and its potential as phosphate-based fertilizer substitute. *Bioresource Technology* **215**, 209–214.

Li, L., Pang, H., He, J. & Zhang, J. 2019 Characterization of phosphorus species distribution in waste activated sludge after anaerobic digestion and chemical precipitation with Fe^{3+} and Mg^{2+}. *Chemical Engineering Journal* **373**, 1279–1285. https://doi.org/10.1016/j.cej.2019.05.146.

Li, X., Zhao, X., Zhou, X. & Yang, B. 2021 Phosphate recovery from aqueous solution via struvite crystallization based on electrochemical-decomposition of nature magnesite. *Journal of Cleaner Production* **292**, 126039. https://doi.org/10.1016/j.jclepro.2021.126039.

Linares-Hernández, I., Barrera-Díaz, C., Bilyeu, B., Juárez-GarcíaRojas, P. & Campos-Medina, E. 2010 A combined electrocoagulation–electrooxidation treatment for industrial wastewater. *Journal of Hazardous Materials* **175** (1–3), 688–694. https://doi.org/10.1016/j.jhazmat.2009.10.064.

Makwana, A. R. & Ahammed, M. M. 2017 Electrocoagulation process for the post-treatment of anaerobically treated urban wastewater. *Separation Science and Technology* **52** (8), 1412–1422.

Mehta, C. M., Khunjar, W. O., Nguyen, V., Tait, S. & Batstone, D. J. 2015 Technologies to recover nutrients from waste streams: A critical review. *Critical Reviews in Environmental Science and Technology* **45** (4), 385–427.

Moerman, W., Carballa, M., Vandekerckhove, A., Derycke, D. & Verstraete, W. 2009 Phosphate removal in agro-industry: Pilot- and full-scale operational considerations of struvite crystallization. *Water Research* **43** (7), 1887–1892.

Monea, M. C., Löhr, D. K., Meyer, C., Preyl, V., Xiao, J., Steinmetz, H., Schönberger, H. & Drenkova-Tuhtan, A. 2020 Comparing the leaching behavior of phosphorus, aluminum and iron from post-precipitated tertiary sludge and anaerobically digested sewage sludge aiming at phosphorus recovery. *Journal of Cleaner Production* **247**, 119129. https://doi.org/10.1016/j.jclepro.2019.119129.

Petzet, S., Peplinski, B. & Cornel, P. 2012 On wet chemical phosphorus recovery from sewage sludge ash by acidic or alkaline leaching and an optimized combination of both. *Water Research* **46** (12), 3769–3780.

Phalakornkule, C., Polgumhang, S. & Tongdaung, W. 2009 Performance of an electrocoagulation process in treating direct dye: batch and continuous upflow processes. *International Journal of Chemical and Molecular Engineering* **3** (9), 499–504.

Ramcharan, T. & Bissessur, A. 2017 Treatment of laundry wastewater by biological and electrocoagulation methods. *Water Science and Technology* **75** (1), 84–93.

Sengupta, S., Nawaz, T. & Beaudry, J. 2015 Nitrogen and phosphorus recovery from wastewater. *Current Pollution Reports* **1** (3), 155–166. https://doi.org/10.1007/s40726-015-0013-1.

Shankar, R., Singh, L., Mondal, P. & Chand, S. 2014 Removal of COD, TOC, and color from pulp and paper industry wastewater through electrocoagulation. *Desalination and Water Treatment* **52** (40–42), 7711–7722. https://doi.org/10.1080/19443994.2013.831782.

Shao, J., Lee, D. H., Yan, R., Liu, M., Wang, X., Liang, D. T., White, T. J. & Chen, H. 2007 Agglomeration characteristics of sludge combustion in a bench-scale fluidized bed combustor. *Energy & Fuels* **21** (5), 2608–2614. https://doi.org/10.1021/ef070004q.

Sincero, A. P. & Sincero, G. A. 2003 Physical-chemical treatment of water and wastewater. IWA Pub, London.

Sridhar, R., Sivakumar, V., Prince Immanuel, V. & Prakash Maran, J. 2011 Treatment of pulp and paper industry bleaching effluent by electrocoagulant process. *Journal of Hazardous Materials* **186** (2), 1495–1502. https://doi.org/10.1016/j.jhazmat.2010.12.028.

Tran, N., Drogui, P., Blais, J.-F. & Mercier, G. 2012 Phosphorus removal from spiked municipal wastewater using either electrochemical coagulation or chemical coagulation as tertiary treatment. *Separation and Purification Technology* **95**, 16–25. https://doi.org/10.1016/j.seppur.2012.04.014.

Wan, J., Wu, B. & Lo, I. M. C. 2020 Development of $Fe0/Fe_3O_4$ composites with tunable properties facilitated by $Fe2+$ for phosphate removal from river water. *Chemical Engineering Journal* **388**, 124242. https://doi.org/10.1016/j.cej.2020.124242.

Wang, L., Skjevrak, G., Hustad, J. E. & Grønli, M. G. 2012 Sintering characteristics of sewage sludge ashes at elevated temperatures. *Fuel Processing Technology* **96**, 88–97. https://doi.org/10.1016/j.fuproc.2011.12.022.

Wang, D., Guo, F., Wu, Y., Li, Z. & Wu, G. 2018 Technical, economic and environmental assessment of coagulation/filtration tertiary treatment processes in full-scale wastewater treatment plants. *Journal of Cleaner Production* **170**, 1185–1194. https://doi.org/10.1016/j.jclepro.2017.09.231.

Ye, Y., Ngo, H. H., Guo, W., Liu, Y., Chang, S. W., Nguyen, D. D., Ren, J., Liu, Y. & Zhang, X. 2019 Feasibility study on a double chamber microbial fuel cell for nutrient recovery from municipal wastewater. *Chemical Engineering Journal* **358**, 236–242. https://doi.org/10.1016/j.cej.2018.09.215.

Yin, J., Zhang, P., Li, F., Li, G. & Hai, B. 2015 Simultaneous biological nitrogen and phosphorus removal with a sequencing batch reactor–biofilm system. *International Biodeterioration & Biodegradation* **103**, 221–226. https://doi.org/10.1016/j.ibiod.2015.02.019.

Yuan, Z., Pratt, S. & Batstone, D. J. 2012 Phosphorus recovery from wastewater through microbial processes. *Current Opinion in Biotechnology* **23** (6), 878–883.

Zeng, J., Ji, M., Zhao, Y., Helmer Pedersen, T. & Wang, H. 2021 Optimization of electrocoagulation process parameters for enhancing phosphate removal in a biofilm-electrocoagulation system. *Water Science and Technology* **83** (10), 2560–2574. https://doi.org/10.2166/wst.2021.132.

Zhang, X., Lin, H. & Hu, B. 2016 Phosphorus removal and recovery from dairy manure by electrocoagulation. *RSC Advances* **6** (63), 57960–57968. https://doi.org/10.1039/C6RA06568F.

Zhang, J., Bligh, M. W., Liang, P., Waite, T. D. & Huang, X. 2018 Phosphorus removal by in situ generated Fe(II): Efficacy, kinetics and mechanism. *Water Research* **136**, 120–130.

First received 24 May 2022; accepted in revised form 28 July 2023. Available online 11 August 2023